Global NEST Journal, Vol 26, No 9, 06546

The effect of artificial metakaolin coarse aggregate on the mechanical and durability properties of lightweight geopolymer concrete

Easwaran P.[1,*], Ramesh S.[2], and Deepanraj C.G.[1]
[1]Department of Civil Engineering, Vivekanandha College of Technology for Women, Elayampalayam, Namakkal - 637 205, India.
[2]Department of Civil Engineering, K.S.Rangasamy College of Technology, Tiruchengode, Namakkal - 637 215, India
Received: 27/07/2024, Accepted: 05/10/2024, Available online: 08/10/2024
*to whom all correspondence should be addressed: e-mail: ereaswarance06@gmail.com
https://doi.org/10.30955/gnj.06546

Graphical abstract

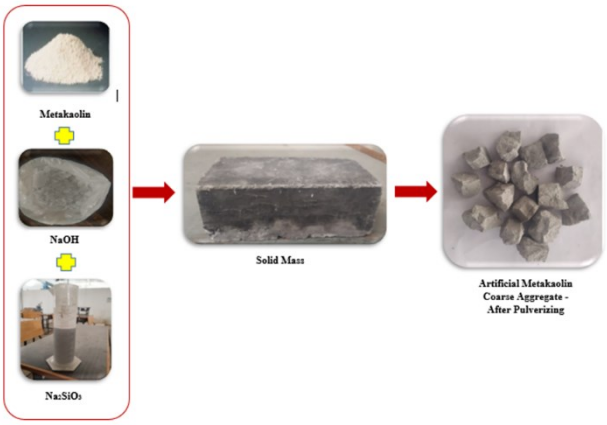

Abstract

This study presents a unique methodology for investigating the properties of Metakaolin Coarse Aggregates (MCA). The NaOH ratios were varied as 8M, 10M, 12M, and 14M, while the NaOH to Na_2SiO_3 ratio was maintained at 0.5 entire study. The liquid-to-binder (L/B) ratios set at 0.3, 0.35, and 0.4. Testing was conducted on the MCA to determine its physical and mechanical properties, comparing them with those of Natural Coarse Aggregate (NCA). Notably, the 8M mix with a 0.4 L/B ratio was found to be economical for producing MCA and was selected for further research. This chosen mix was then employed to prepare geopolymer concrete with 50% MK and 50% PA, with L/B ratios set at 0.4, 0.45, and 0.5. The NaOH ratio and Na_2SiO_3 to NaOH ratio were maintained at a constant 8M and 2, respectively. Mechanical and durability properties were compared between Geopolymer concrete with NCA and Geopolymer concrete with MCA. The test results demonstrate that MCA in geopolymer concrete can effectively replace NCA in geopolymer concrete, making it a viable option for structural members. Additionally, microstructural characterization was performed on Geopolymer concrete with MCA mixes with varying L/B ratios of 0.4, 0.45, and 0.5, at 28 days. The study specifically focuses on the Interfacial Transition Zone (ITZ) between MCA and geopolymer paste, revealing an improvement in ITZ and microstructure in the GMCA sample with a 0.4 L/B ratio compared to other mixes.

Keywords: Metakaolin coarse aggregate, geopolymer concrete, mechanical properties, durability properties, microstructure analysis

1. Introduction

The nature of geopolymer concrete is best understood as a composite material with two distinct phases: the binder and aggregate phase (Ralli and Pantazopoulou, 2004). The production of geopolymeric binders is triggered through the interaction of aluminosilicate-rich source materials. These source materials include fly ash (Hardjito *et al.* 2004), GGBS (Kumar *et al.* 2018), metakaolin (Mohmmad *et al.* 2023), rice husk ash (Pham *et al.* 2021), silica fume (Okoye *et al.* 2017), pond ash (Yuvaraj and Ramesh, 2022), and Alccofine 1203 (Sagar and Sivakumar, 2021), all of which contribute to the production of these binders. Employing geopolymer binders presents an opportunity to decrease the reliance on ordinary cement and effectively repurpose various waste materials that are typically disposed of in landfills, thereby addressing multiple environmental concerns (Kipsanai *et al.* 2021). Explorations into geopolymer concrete thus far have showcased its exceptional qualities, positioning it as a promising material for construction purposes (Golafshani *et al.* 2024). In geopolymer concrete (GPC), the aggregate phase, comprising both fine and coarse shape, represents the largest portion of the total volume (Albidah *et al.* 2021). The extensive utilization of aggregates is projected to reach 62.9 billion metric tons annually by 2024, raising significant environmental concerns due to the potential reduction of natural resources. (Un *et al.* 2015). The responsiveness of the sand aggregate is a crucial factor influencing the development of geopolymeric binders, influencing the alkali activation processes within the GPC (Prasad *et al.* 2021).

Geopolymer concrete produced with both natural aggregate (Pawluczuk *et al.* 2021; Kalinowska-Wichrowska *et al.* 2022) and artificial aggregates (Xu *et al.* 2021; Qian *et al.* 2021 ; Priyanka *et al.* 2020), aiming to achieve favorable mechanical and durability outcomes. Conversely, the natural aggregate properties significantly improve mechanical aspects (Lima *et al.* 2013). In terms of artificial aggregate production techniques, researchers predominantly employ two methods: crushing (Wang *et al.* 2023; Cioffi *et al.* 2013) and pelletization (Zheng *et al.* 2021; Verma *et al.* 2022). The initial approach involves directly crushing geopolymer pastes into jagged pieces, making it the viable method for large-scale industry (Bekkeri *et al.* 2023). The arrangement and form of the artificial aggregate primarily determine the packing within the mixture. A densely packed aggregate may lead to a decrease in the geopolymer binder layer coating on the particles, resulting in reduced workability of the mixture (Baskar *et al.* 2023). Conversely, in the pelletization techniques, artificial aggregates with round shapes can be generated utilizing a rotating disc (Guneyisi *et al.* 2016). Mechanical parameters (e.g., speed, angle) significantly influence density and strength of lightweight aggregate from industrial by-products (e.g., sewage sludge (Franus *et al.* 2015)), agricultural wastes (e.g., rice husk ash (Gonzalez-Corrochano *et al.* 2009) and sugarcane straw ash (Jalal *et al.* 2021)). Speed and angle of the disc affect water absorption; moisture content and raw material grain size distribution determine aggregate size attainment (Alqahtani *et al.* 2018). The presence of numerous voids in lightweight concrete contributes to shrinkage, promoting diminishing strength (Zong *et al.* 2014; Liu *et al.* 2014). The discovery of lightweight aggregate has been crucial for lightweight concrete, reducing building emissions and structural weight. Using it enhances thermal insulation, cuts dead load, enables larger structures on the same foundation, and lowers CO_2 emissions (Liu *et al.* 2018).

Several research endeavors have delved into the preparation of lightweight aggregates, employing methods like sintering (Lo *et al.* 2016; Mohan and Vasudev, 2018), cold bonding (Tajra *et al.* 2018; Wang *et al.* 2020), or autoclaving processes (Nadesan and Dinakar, 2018) with industrial by-products. Though the sintering method requires significant energy, its engineering properties are notable when applied to specific mix designs. The sintering process stands out as widely utilized techniques for the mass manufacture of aggregates, eliminating the need for an extended curing process (Guneyisi *et al.* 2013). In contrast, the cold bonding techniques is seen as economical since it solidifies at ambient heat. However, a major challenge is the need for an extended 28-day curing period before the aggregates can be used in construction (George and Revathi 2020). An autoclave machine, set to specific temperature and pressure levels, creates aggregates that harden rapidly. This method requires only a small amount of binding material and a short curing time, making it efficient and effective. Various researchers highlight the strong bonding between geopolymer binders and aggregates (Ren and Zhang, 2018). The Interfacial Transition Zone (ITZ), recognized as interface in concrete, exists between the cement paste and aggregate in ordinary concrete (Hajimohammadi *et al.* 2019). The failure of traditional natural aggregate in concrete, heavily influenced by matrix and ITZ characteristics, is often determined by the properties of the geopolymer aggregate in geopolymer concrete (Ollivier *et al.* 1995). Unlike natural aggregates, which are commonly considered inert, geopolymer aggregates react with cementitious matrix, thereby enhancing the characteristics (Vargas *et al.* 2017).

Based on the aforementioned context, the objective of this study is to explore the effect of artificial metakaolin coarse aggregate on the mechanical and durability properties of lightweight geopolymer concrete. Metakaolin, a premium-grade pozzolan, results from heating kaolin clay at temperatures ranging from 600 to 850°C. In this study, metakaolin was employed for the production of Metakaolin Coarse Aggregate (MCA). Metakaolin reacts with the alkaline solution, resulting in the formation of a solid mass. This geopolymeric mass was manually pulverized to create MCA. The primary objective of the experiment was to assess the performance of MCA in comparison to natural coarse aggregate. Through this comparison, the optimal geopolymer mix for MCA was determined. The optimal mix of MCA was employed to create Geopolymer concrete with Metakaolin Coarse Aggregate (GMCA), which was then compared with Geopolymer concrete with Natural Coarse Aggregate (GNCA). Comprehensive investigations were conducted on mechanical properties of GNCA and GMCA with various liquid to binder ratios, encompassing parameters such as density and compressive strength. Additionally, the durability properties were thoroughly examined through tests including ultrasonic pulse velocity, rapid chloride penetration, and sorptivity. Furthermore, it was advisable to conduct a microstructural examination of the internal composition of the material. This can offer insights into geopolymer phase distribution, particle bonding, the existence of gaps or faults, and overall homogeneity.

2. Production of artificial metakaolin coarse aggregate

Metakaolin coarse aggregates (MCA) were produced through the blending of metakaolin with varying molarity (8M to 14M) and liquid-to-binder ratios (0.3, 0.35 and 0.4). An alkaline solution was prepared for the entire study, characterized by a sodium silicate to sodium hydroxide (Na_2SiO_3/NaOH) mass ratio of 2.0 and a sodium hydroxide to sodium silicate (NaOH/Na_2SiO_4) ratio set at 0.5 (Ankur and Rafat, 2018). The initial step involves the thorough mixing of metakaolin with the alkaline solution. Following this, the mixes were poured into the mold and cured with ambient curing and then pulverization to allow 20 mm MCA. The production process of MCA as shown in Figure 1 and the various mix proportions were employed in the production of MCA and were documented in Table 1.

2.1. Physical and mechanical properties

Table 2 displays the physical properties of both MCA and NCA. The specific gravity of $^{8}MCA_{0.3}$, $^{8}MCA_{0.35}$, and $^{8}MCA_{0.4}$ ranges between 2.14 and 2.15, exhibiting a 20.44% reduction than NCA. Similarly, the specific gravity of $^{10}MCA_{0.3}$, $^{10}MCA_{0.35}$, and $^{10}MCA_{0.4}$ lies within the range of

2.20 to 2.21, indicating an 18.21% decrease in comparison to NCA. For $^{12}MCA_{0.3}$, $^{12}MCA_{0.35}$, and $^{12}MCA_{0.4}$, the specific gravity ranges from 2.18 to 2.19, showcasing an 18.95% decrease than NCA. Lastly, the specific gravity of $^{14}MCA_{0.3}$, $^{14}MCA_{0.35}$, and $^{14}MCA_{0.4}$ ranges from 2.17 to 2.20, reflecting a 19.33% reduction than NCA.

Table 1. Proportions for production of artifical MCA

Mix id	NaOH (M)	Liquid to metakaolin ratio	$NaOH/Na_2SiO_4$ ratio
$^{8}MCA_{0.3}$	8	0.3	0.5
$^{8}MCA_{0.35}$	8	0.35	0.5
$^{8}MCA_{0.4}$	8	0.4	0.5
$^{10}MCA_{0.3}$	10	0.3	0.5
$^{10}MCA_{0.35}$	10	0.35	0.5
$^{10}MCA_{0.4}$	10	0.4	0.5
$^{12}MCA_{0.3}$	12	0.3	0.5
$^{12}MCA_{0.35}$	12	0.35	0.5
$^{12}MCA_{0.4}$	12	0.4	0.5
$^{14}MCA_{0.3}$	14	0.3	0.5
$^{14}MCA_{0.35}$	14	0.35	0.5
$^{14}MCA_{0.4}$	14	0.4	0.5

Table 2. Physical and mechanical properties of NCA and MCA

Test on aggregate	NCA	$^{8}MCA_{0.3}$	$^{8}MCA_{0.35}$	$^{8}MCA_{0.4}$	$^{10}MCA_{0.3}$	$^{10}MCA_{0.35}$	$^{10}MCA_{0.4}$	$^{12}MCA_{0.3}$	$^{12}MCA_{0.35}$	$^{12}MCA_{0.4}$	$^{14}MCA_{0.3}$	$^{14}MCA_{0.35}$	$^{14}MCA_{0.4}$
SG	2.69	2.15	2.14	2.15	2.20	2.21	2.20	2.18	2.19	2.19	2.17	2.18	2.20
FM	6.73	6.57	6.12	6.35	6.22	6.46	6.15	6.69	6.55	6.13	6.34	6.58	6.52
BD (Kg/m^3)	1550	1073	1072	1071	1073	1074	1072	1071	1072	1072	1072	1073	1075
FI (%)	16	12	14	13	14	13	13	14	14	15	15	14	15
WA (%)	0.45	1.84	1.87	1.82	1.86	1.85	1.82	1.85	1.88	1.88	1.83	1.82	1.85
IV (%)	18.7	13.5	12.2	14.8	15.1	12.6	14.7	10.4	14.8	13.6	17.0	15.5	12.3
CT (%)	27	26.7	24.2	25.5	25.8	16.5	22.6	26.4	24.7	18.6	25.3	26.5	23.1
AT (%)	33	22	21	20	23	20	22	24	25	23	24	23	21

SG: Specific Gravity; FM : Fineness Modulus; BD: Bulk Density; FI : Flakiness Index; WA: Water Absorption; IV: Impact Value; CT: Crushing Test; AT: Abrasion Test

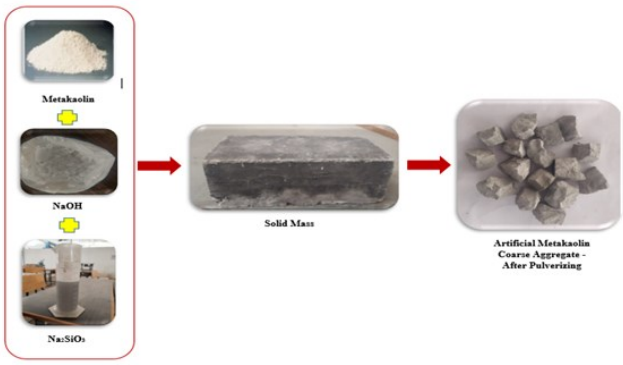

Figure 1. The production process of artifical MCA

The MCA produced in this study exists as a 20 mm aggregate. The fineness modulus of $^{8}MCA_{0.3}$, $^{8}MCA_{0.35}$, and $^{8}MCA_{0.4}$ spans from 6.12 to 6.57, showcasing a 9.06% decrease than NCA. Similarly, the fineness modulus of $^{10}MCA_{0.3}$, $^{10}MCA_{0.35}$, and $^{10}MCA_{0.4}$ falls within the range of 6.15 to 6.46, indicating an 8.61% reduction than NCA. For $^{12}MCA_{0.3}$, $^{12}MCA_{0.35}$, and $^{12}MCA_{0.4}$, the fineness modulus ranges from 6.13 to 6.69, demonstrating an 8.91% decrease than NCA. Lastly, the fineness modulus of $^{14}MCA_{0.3}$, $^{14}MCA_{0.35}$, and $^{14}MCA_{0.4}$ ranges from 6.34 to 6.58, reflecting a 5.79% reduction than NCA.

For NCA, the bulk density was recorded as 1,550 kg/m^3. In contrast, the bulk density of the $^{8}MCA_{0.3}$, $^{8}MCA_{0.35}$, and $^{8}MCA_{0.4}$, prepared in this study, ranges from 1071 to 1073 kg/m^3, respectively. Similarly, the bulk density of the $^{10}MCA_{0.3}$, $^{10}MCA_{0.35}$, and $^{10}MCA_{0.4}$ is in the range of 1072 to 1074 kg/m^3. Additionally, the bulk density of the $^{12}MCA_{0.3}$, $^{12}MCA_{0.35}$, and $^{12}MCA_{0.4}$ ranges from 1071 to 1072 kg/m^3, while that of $^{14}MCA_{0.3}$, $^{14}MCA_{0.35}$, and $^{14}MCA_{0.4}$ varies from 1072 to 1075 kg/m^3. These findings indicate that the bulk density of MCA is consistently lower than that of NCA, aligning with IS: 9142–1979.

The flakiness index for NCA was recorded at 16%. In comparison, the flakiness index for $^{8}MCA_{0.3}$, $^{8}MCA_{0.35}$, and $^{8}MCA_{0.4}$, falls within the range of 12 to 14%. Similarly, the flakiness index for $^{10}MCA_{0.3}$, $^{10}MCA_{0.35}$, and $^{10}MCA_{0.4}$ is in the range of 13 to 14%. Additionally, the flakiness index for $^{12}MCA_{0.3}$, $^{12}MCA_{0.35}$, and $^{12}MCA_{0.4}$ ranges from 14 to 15%, while that of $^{14}MCA_{0.3}$, $^{14}MCA_{0.35}$, and $^{14}MCA_{0.4}$ falls within the range of 14 to 15%. To comply with the IS 2386 Part I standards, it was advised that the flakiness value for NCA should be below 25%. For MCA, this requirement is duly fulfilled.

The 24-hour water absorption for NCA was determined to be 0.45%. In contrast, the water absorption for $^{8}MCA_{0.3}$, $^{8}MCA_{0.35}$, and $^{8}MCA_{0.4}$ ranges from 1.82 to 1.84%. Similarly,

the water absorption for $^{10}MCA_{0.3}$, $^{10}MCA_{0.35}$, and $^{10}MCA_{0.4}$ was within the range of 1.82 to 1.86%. For $^{12}MCA_{0.3}$, $^{12}MCA_{0.35}$, and $^{12}MCA_{0.4}$, the water absorption ranges from 1.85 to 1.88%. Lastly, the water absorption of $^{14}MCA_{0.3}$, $^{14}MCA_{0.35}$, and $^{14}MCA_{0.4}$ spans from 1.82 to 1.85%. The results indicate that MCA exhibits higher water absorption values were compared to NCA; however, these values still adhere to the IS 2386 Part III standards. Therefore, MCA was deemed suitable for use in concrete applications and is recommended accordingly.

The impact value for concrete should not exceed 30% by weight as per IS 383 - 2016 Part IV. For NCA, the impact value is measured at 18.7%. Conversely, the impact value for $^{8}MCA_{0.3}$, $^{8}MCA_{0.35}$, and $^{8}MCA_{0.4}$ flies within the range of 12.2 to 14.8%. Similarly, the impact value for $^{10}MCA_{0.3}$, $^{10}MCA_{0.35}$, and $^{10}MCA_{0.4}$ ranges from 12.6 to 15.1%. Furthermore, the impact value for $^{12}MCA_{0.3}$, $^{12}MCA_{0.35}$, and $^{12}MCA_{0.4}$ ranges from 10.4 to 14.8%. Lastly, the impact value for $^{14}MCA_{0.3}$, $^{14}MCA_{0.35}$, and $^{14}MCA_{0.4}$ spans from 12.3 to 17.0%. Given that the impact value of MCA remains below 30%, it is highly recommended for use in runways, pavements, and roads due to its favorable characteristics.

In line with IS: 383 – 2016 Part IV, the crushing value for concrete should not exceed 30% by weight. NCA exhibits a crushing value of 27%, which is lower than that of $^{8}MCA_{0.3}$, $^{8}MCA_{0.35}$, and $^{8}MCA_{0.4}$, ranging from 24.2 to 26.7%. Similarly, the crushing value for $^{10}MCA_{0.3}$, $^{10}MCA_{0.35}$, and $^{10}MCA_{0.4}$ was within the range of 26.5 to 25.8%. For $^{12}MCA_{0.3}$, $^{12}MCA_{0.35}$, and $^{12}MCA_{0.4}$, the crushing value ranges from 18.6 to 26.4%, while for $^{14}MCA_{0.3}$, $^{14}MCA_{0.35}$, and $^{14}MCA_{0.4}$, it is in the range of 23.1 to 26.5%. The consistent maintenance of an impact value below 30% for MCA strongly recommends its application in wearing surfaces.

In accordance with IS 383 – 2016 Part IV, the aggregate abrasion value for aggregates used in non-wearing surfaces of concrete should not exceed 50% by weight. Notably, NCA exhibits an abrasion value of 33%, which was lower than that of $^{8}MCA_{0.3}$, $^{8}MCA_{0.35}$, and $^{8}MCA_{0.4}$, ranging from 20 to 22%. Similarly, the abrasion value for $^{10}MCA_{0.3}$, $^{10}MCA_{0.35}$, and $^{10}MCA_{0.4}$ lies within the range of 20 to 23%. For $^{12}MCA_{0.3}$, $^{12}MCA_{0.35}$, and $^{12}MCA_{0.4}$, the abrasion value ranges from 23 to 25%, while for $^{14}MCA_{0.3}$, $^{14}MCA_{0.35}$, and $^{14}MCA_{0.4}$, it was in the range of 21 to 24%. The decrease in abrasion value for MCA than NCA indicates that MCA was more resistant to abrasive loads.

After comprehensive evaluation of the physical and mechanical properties of all MCA mixes, a judicious decision was made to select 8M NaOH, considering it is the most expensive component in these mixes and addressing economic considerations. It was evident that the properties of $^{8}MCA_{0.4}$ mix align with the standards specified in IS: 383 – 2016. Consequently, $^{8}MCA_{0.4}$ was chosen for further studies.

2.2. Test methods

The compressive strength of geopolymer concrete, with 150 mm cube specimens, was evaluated at 7, 28, and 90 days by substituting natural coarse aggregate (NCA) with metakaolin coarse aggregate (MCA), in accordance with IS: 516 – 1989 guidelines. The compressive strength of Geopolymer concrete with Natural Coarse Aggregate (GNCA) and Geopolymer concrete with Metakaolin Coarse Aggregate (GMCA) was assessed at various L/B ratios of 0.4, 0.45, and 0.5. Ultrasonic Pulse Velocity (UPV) tests were performed before the compressive strength assessments at 7, 28, and 90 days, following IS 13311 (Part 1): 1992 procedures. The UPV of GNCA and GMCA at different L/B ratios (0.4, 0.45, and 0.5) was measured at these ages. Rapid Chloride Penetration Tests (RCPT) were conducted in accordance with ASTM C1202 - 17 at 7, 28, and 90 days for both GNCA and GMCA, using 100 mm diameter by 50 mm thick cylindrical specimens. A comparative analysis of RCPT values was performed for both GNCA and GMCA across the different L/B ratios. Additionally, Sorptivity tests (ST) were executed following ASTM C 1585 - 04 guidelines at all ages (7, 28, and 90 days) for both GNCA and GMCA, using 100 mm diameter by 50 mm thick cylindrical specimens. The comparative analysis of ST values was conducted for both GNCA and GMCA at different L/B ratios. The microstructure of $GMCA_{0.4}$, $GMCA_{0.45}$, and $GMCA_{0.5}$ samples was examined after a 28-day curing period, with a specific focus on the Interfacial Transition Zone (ITZ), using the TESCAN VEGA3 scanning electron microscope (SEM).

3. Mix proportion of geopolymer concrete with NCA and MCA

The geopolymer concrete (GPC) was made with 50% metakaolin (MK) and 50% pond ash (PA), using an alkaline solution with a (Na_2SiO_4/NaOH) ratio of 2. Different liquid-to-binder (L/B) ratios of 0.4, 0.45, and 0.5 were used. The molarity of NaOH was selected as 8 M. The chemical proportions and properties of MK and PA were as given in Table 3.

Throughout the study, manufactured sand (M-sand) served as the fine aggregate in both GPC with NCA and GPC with MCA concrete. The properties of M-sand and NCA and MCA were given in the Table 4. The optimal mix proportion of MCA for preparing geopolymer concrete with both natural and metakaolin coarse aggregates was detailed in Table 5. In Table 5, the notation "$GNCA_{0.4}$" signifies geopolymer concrete with NCA and an alkaline L/B ratio of 0.4. Similarly, "$GMCA_{0.4}$" represents geopolymer concrete with MCA and an alkaline L/B ratio of 0.4. GMCA mixes were produced and their properties were assessed at intervals of 7, 28, and 90 days. These results were subsequently compared to those of GNCA mixes.

3.1. Production of lightweight geopolymer concrete with NCA and MCA

3.1.1. Density and compressive strength of geopolymer metakaolin coarse aggregate (GMCA)

The density variations of GNCA and GMCA were illustrated in Figure 2. In terms of fresh density, $GMCA_{0.4}$, $GMCA_{0.45}$, and $GMCA_{0.5}$ exhibit density increase ranging from 1820 to 1827 kg/m³, while the density of $GNCA_{0.4}$, $GNCA_{0.45}$, and $GNCA^{0.5}$ varies from 2353 to 2360 kg/m³. For dry hardened density, $GMCA_{0.4}$, $GMCA_{0.45}$, and $GMCA_{0.5}$ show density increase between 1821 to 1831 kg/m³, whereas the density of $GNCA_{0.4}$, $GNCA_{0.45}$, and $GNCA_{0.5}$ varies from 2401 to 2410 kg/m³. Moving to, air-dried density for $GMCA_{0.4}$, $GMCA_{0.45}$, and $GMCA_{0.5}$ sees a rise between 1755 to 1767 kg/m³, while

the density of $GNCA_{0.4}$, $GNCA_{0.45}$, and $GNCA_{0.5}$ varies from 2348 to 2369 kg/m³. In terms of oven-dry density, $GMCA_{0.4}$, $GMCA_{0.45}$, and $GMCA_{0.5}$ experience density increase between 1718 to 1732 kg/m³, whereas the density of $GNCA_{0.4}$, $GNCA_{0.45}$, and $GNCA_{0.5}$ varies from 2311 to 2320 kg/m³. The oven-dry densities of $GMCA_{0.4}$, $GMCA_{0.45}$, and $GMCA_{0.5}$ were significantly lower than those of $GNCA_{0.4}$, $GNCA_{0.45}$, and $GNCA_{0.5}$ due to the large water absorption capacity inherent in MCA. The test results indicate that the densities of $GMCA_{0.4}$, $GMCA_{0.45}$, and $GMCA_{0.5}$ were lower than those of $GNCA_{0.4}$, $GNCA_{0.45}$, and $GNCA_{0.5}$. This characteristic classifies them as lightweight aggregate concrete, as provided by (Sata *et al.* 2007). This pattern is influenced by the lower bulk density of MCA (1071 kg/m³) compared to NCA (1550 kg/m³). The rise in density can be linked to greater amount of silica source materials, contributing to the formation of a more bonded microstructure (Chindaprasirt, 2020).

Table 3. Chemical proportions and properties of MK and PA

Elements	Oxides (%)	
	MK	PA
SiO_2	50.15	51.18
Al_2O_3	43.02	29.72
Fe_2O_3	0.65	7.09
CaO	0.23	0.89
MgO	0.07	0.87
SO_3	0.75	4.28
LOI	7.34	4.01
Specific gravity	2.60	2.17
Specific surface area (m^2/kg)	2000	398

Table 4. Properties of M-sand and NCA and artificial MCA

Properties	M-sand	NCA	MCA
Fineness modulus	2.46	6.71	6.35
Specific gravity	2.71	2.69	2.15
Absorption (%)	1.00	0.5	1.82
Bulk density (kg/m³)	1555	1697	1071

Table 5. Mix proportions of GNCA and GMCA

Mix id	Materials (kg/m³)							
	MK	PA	Fine aggregate	Coarse aggregate		NaOH	Na_2SiO_4	Na_2SiO_4 / NaOH
				NCA	MCA			
$GNCA_{0.4}$	200	200	540	1260	1260	57.16	114.33	2
$GMCA_{0.4}$	200	200	540	1260	1260	57.16	114.33	2
$GNCA_{0.45}$	200	200	540	1260	1260	62.07	124.14	2
$GMCA_{0.45}$	200	200	540	1260	1260	62.07	124.14	2
$GNCA_{0.5}$	200	200	540	1260	1260	66.67	133.34	2
$GMCA_{0.5}$	200	200	540	1260	1260	66.67	133.34	2

GNCA : Geopolymer concrete with NCA; GMCA : Geopolymer concrete with MCA ; 0.40 , 0.45 and 0.5 : Liquid to binder (L/B) ratios

In Figure 3, At 7 days of age, $GMCA_{0.4}$, $GMCA_{0.45}$, and $GMCA_{0.5}$ exhibit compressive strengths that were 2.58%, 1.41%, and 0.82% higher, respectively, than the corresponding strengths of $GNCA_{0.4}$, $GNCA_{0.45}$, and $GNCA_{0.5}$. By the 28th day, $GMCA_{0.4}$ demonstrates the compressive strength 2.28% higher than $GNCA_{0.4}$, while $GMCA_{0.45}$ and $GMCA_{0.5}$ exhibit strengths 1.00% and 0.67% higher than $GNCA_{0.45}$ and $GNCA_{0.5}$, respectively. The compressive strength of $GMCA_{0.4}$, $GMCA_{0.45}$, and $GMCA_{0.5}$ at 90 days was also respectively 2.18%, 0.78%, and 0.48% higher than $GNCA_{0.4}$, $GNCA_{0.45}$, and $GNCA_{0.5}$. The early strength development in lightweight concrete was evident when utilizing lightweight aggregates with geopolymer (Hao *et al.* 2022). The experimental findings indicate that $GMCA_{0.4}$ concrete demonstrates greater compressive strength than $GMCA_{0.45}$ and $GMCA_{0.5}$. The observed phenomenon promotes voids nature of MCA, fostering enhanced bonding between the mortar paste and the ITZ. This potentially explains the slight promotion in the compressive strength of GMCA. Additionally, the high angularity of MCA facilitates better packing of the aggregates, potentially contributing to the increment in strength aspect. The variations in strength across mixtures with different L/B ratios and aggregate parameters are primarily attributed to differences in microstructure and ITZ characteristics. Analyzing the role of aggregate voids, packing efficiency, and the interaction between the geopolymer matrix and the ITZ can provide a comprehensive understanding of these strength variations (Peng *et al.* 2020). The reduction in the L/B ratio resulted in the highest compressive strength at all ages. This aligns with findings by (Peng *et al.* 2021), where it was reported that a lower L/B ratio enhances compressive strength in blended fly ash and MK with GPM.

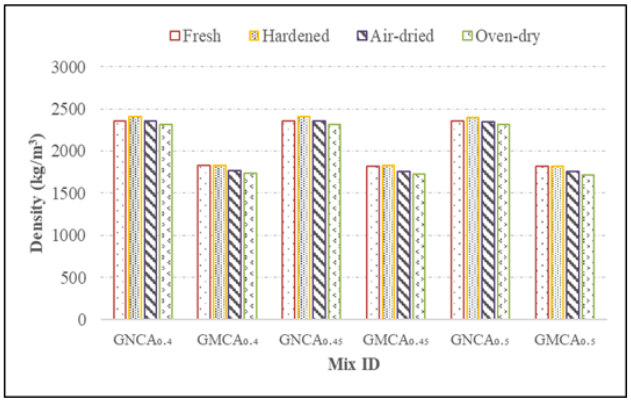

Figure 2. Density variations of GNCA and GMCA with various L/B ratios

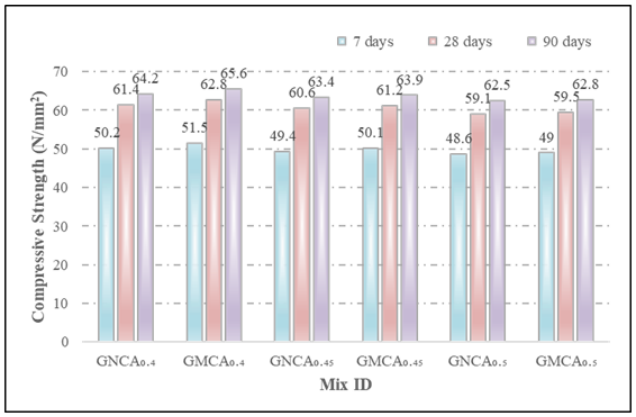

Figure 3. Compressive strength of GNCA and GMCA with various L/B ratios

3.1.2. Durability properties of geopolymer metakaolin coarse aggregate concrete (GMCA)

In Figure 4, At 7 days of age, $GMCA_{0.4}$, $GMCA_{0.45}$, and $GMCA_{0.5}$ exhibit UPV ranging from 4.1 to 4.3 km/s. By the 28th day, $GMCA_{0.4}$, $GMCA_{0.45}$, and $GMCA_{0.5}$ demonstrated velocity ranging from 4.3 to 4.5 km/s. Furthermore, at 90 days of age, $GMCA_{0.4}$, $GMCA_{0.45}$, and $GMCA_{0.5}$ exhibit velocity ranges from 4.4 to 4.55 km/s. All these values were classified as "Good" according to IS 13311 (Part I): 1992. The UPV of MCA exceeded that of NCA at all ages. This phenomenon can be linked to the reduction in the ITZ gap due to the angular shape of MCA and paste. This reduction provides a path for micro cracks to interconnect, resulting better strength in GMCA compared to GNCA. Similar trend reported by (Farahani *et al.* 2017; Zhang and Aslani, 2021; Zhuang *et al.* 2016), where it was reported that a reduction in the ITZ gap enhances UPV in concrete.

In Figure 5, At 7 days of age, $GMCA_{0.4}$, $GMCA_{0.45}$, and $GMCA_{0.5}$ exhibit RCPT values varied from 1286 coulombs to 1371 coulombs. By the 28th day, $GMCA_{0.4}$, $GMCA_{0.45}$, and $GMCA_{0.5}$ demonstrated RCPT values varied from 1201 coulombs to 1282 coulombs. Additionally, at 90 days of age, $GMCA_{0.4}$, $GMCA_{0.45}$, and $GMCA_{0.5}$ exhibit RCPT values varied from 1087 coulombs to 1140 coulombs. All these values fall within the "moderate" category according to ASTM C 1202-17. It was noteworthy that as the age increases, the RCPT decreases. This observation indicates that a lesser amount of charge passes through GNCA than GMCA. The increase in chloride permeability is primarily attributed to the porous paste structure resulting from the inclusion of MCA content. Additionally, the rise in L/B ratio leads to higher chloride permeability, reflecting the influence of the porous microstructure of the concrete. This result aligns with the observations made by (Thokchom *et al.* 2009).

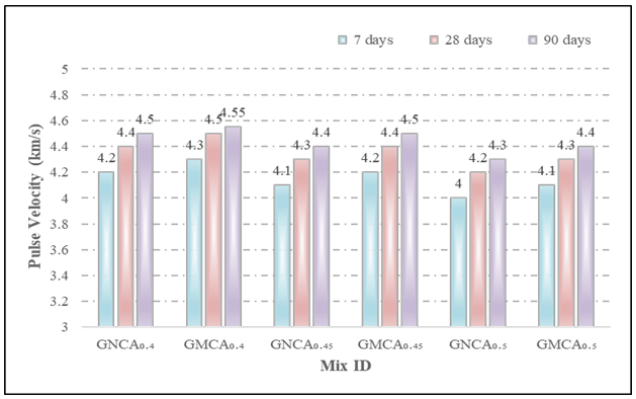

Figure 4. Ultrasonic pulse velocity (UPV) of GNCA and GMCA with various L/B ratios

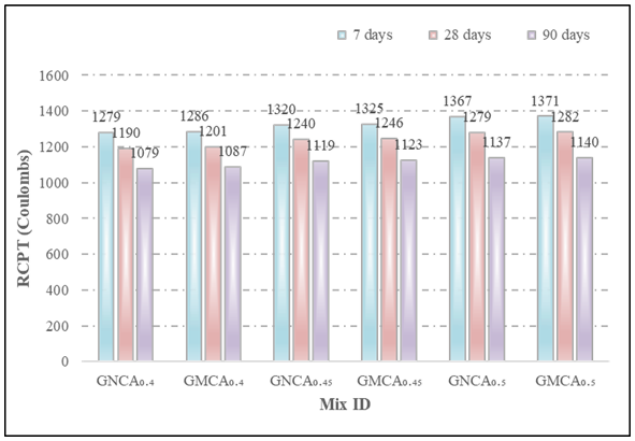

Figure 5. Rapid chloride penetration test (RCPT) of GNCA and GMCA with various L/B ratios

Figure 6 illustrates the comparative analysis of ST values for both GNCA and GMCA at different L/B ratios (0.4, 0.45, and 0.5). At 7 days, the sorptivity (ST) value for $GMCA_{0.4}$ was 0.83 mm/√min x 10^{-4}, representing a 3.75% increase compared to $GNCA_{0.4}$. Similarly, the ST value for $GMCA_{0.45}$ was 0.86 mm/√min x 10^{-4}, indicating a 4.87% increase compared to $GNCA_{0.45}$. $GMCA_{0.5}$ shows an ST value of 0.89 mm/√min x 10^{-4} at 7 days, showcasing a 5.95% increase compared to $GNCA_{0.5}$. At 28 days, the ST value for $GMCA_{0.4}$ was 0.69 mm/√min x 10^{-4}, exhibiting a 3.00% increase compared to $GNCA_{0.4}$. Similarly, the ST value for $GMCA_{0.45}$ was 0.73 mm/√min x 10^{-4}, indicating a 4.10% increase compared to $GNCA_{0.45}$. $GMCA_{0.5}$ shows an ST value of 0.78 mm/√min x 10^{-4} at 28 days, showcasing a 5.40% increase compared to $GNCA_{0.5}$. At 90 days, the ST value for $GMCA_{0.4}$ was 0.58 mm/√min x 10^{-4}, exhibiting a 1.75% increase compared to $GNCA_{0.4}$. Similarly, the ST value for $GMCA_{0.45}$ is 0.62 mm/√min x 10^{-4}, indicating a 3.33% increase compared to $GNCA_{0.45}$. $GMCA_{0.5}$ shows an ST value of 0.64 mm/√min x 10^{-4} at 90 days, showcasing a 4.91% increase compared to $GNCA_{0.5}$. The evident increase in sorptivity in GMCA, when NCA was replaced with MCA, which was ascribed to the highly porous nature of the MCA in

geopolymer concrete. The inclusion of MCA in the geopolymer mix contributes to the formation of a porous paste structure and the less favorable ITZ, leading to higher permeability compared to NCA in geopolymer mix. The augmentation of capillary porous in the concrete matrix, due to the inclusion of MCA, results in increased water absorption through capillary action. These findings are consistent with the observations reported by (Law *et al.* 2015; Xie *et al.* 2019).

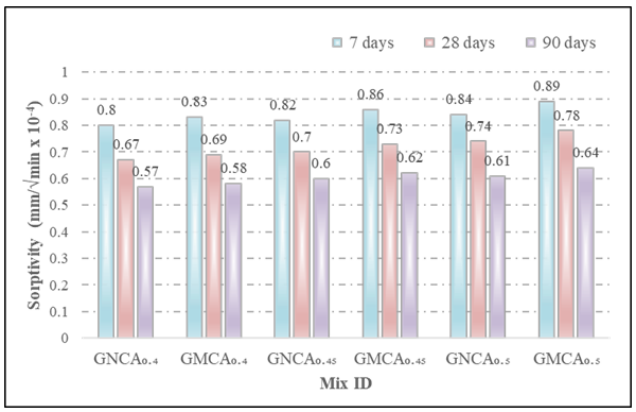

Figure 6. Rapid chloride penetration test (RCPT) of GNCA and GMCA with various L/B ratios

3.2. Microstructural analysis

Figures 7 to 9 depict the ITZ at different L/B ratios in GMCA samples. These images reveal that a decrease in the L/B ratio correlates with abatement in ITZ width. A reduced L/B ratio was associated with an increased concentration of geopolymer gel within the lattice. The particle size converges with that of the ITZ, allowing them to fill the ITZ space and improve its properties. In Figure 7, the arrangement of geopolymer paste and micropores in the concrete significantly impacts its performance. A diminished ITZ width plays a crucial role in preventing premature failure, elucidating the superior compressive strength exhibited by the $GMCA_{0.4}$ sample in comparison to $GMCA_{0.45}$ and $GMCA_{0.5}$. Further, it seems evident that a complete and strong bond exists between the MCA and the geopolymer binder. Figures 8 demonstrate that the existence of voids in the geopolymer paste diminishes concrete strength by creating routes for interconnected micro cracks. The gap between the aggregate and the paste is a consequence of an inadequate polymeric reaction during the maturation process. In Figure 9, an elevated ITZ width was observed, indicating the decrease in the extent of geopolymerization reactions. The increased ITZ width suggests that a reduced amount of geopolymerization reactions occurred, potentially due to higher amounts of water availability hindering the alkali transition process. (Shi *et al.* 2019) noted the creation of CASH and CSH paste at the interface between recycled aggregate and the geopolymer binder. Similarly, Shi *et al.* (Ouda and Gharieb, 2020) identified the presence of CSH in the ITZ. This development improves the mechanical and durability aspects of the system (Ren and Zhang, 2018; Shi *et al.* 2012).

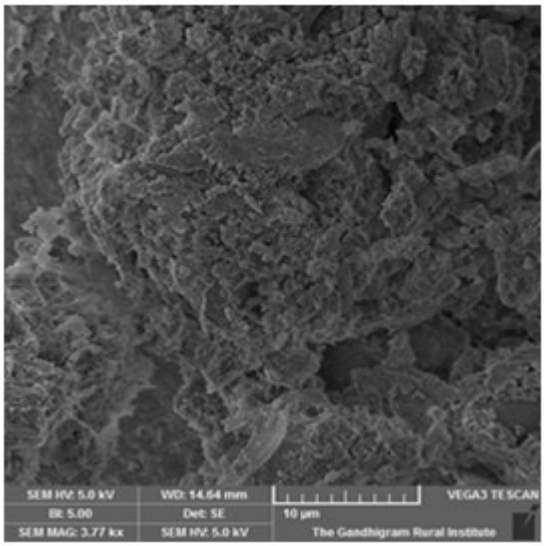

Figure 7. SEM image of $GMCA_{0.4}$ mix

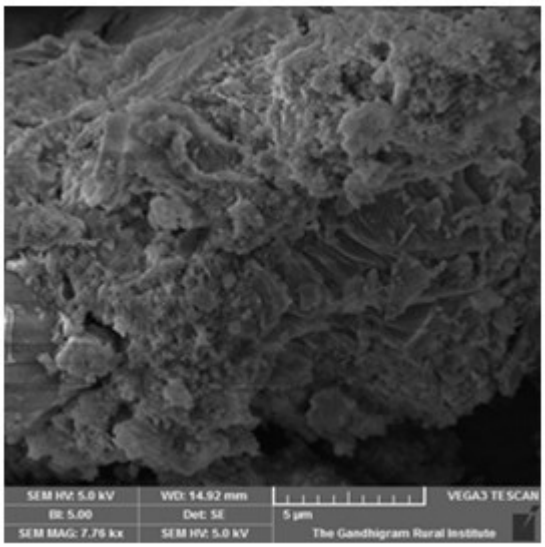

Figure 8. SEM image of $GMCA_{0.45}$ mix

4. Conclusions

This study aimed to test geopolymer concrete with MCA at various L/B ratios. The conclusions based on the experimental results were as follows.

The trial mixes reveal that MCA exhibits the potential to replace NCA. The most cost-effective and efficient mix proportion for MCA preparation was identified as 8M, characterized by an 8 Molar NaOH solution and L/B ratio of 0.4. Since the properties of $^{8}MCA0.4$ meet the specifications outlined in IS: 383 – 2016, it was deemed the optimal outcome among all mixes, considering economic factors.

The fresh, hardened, air-dried, and oven-dry densities of $GMCA_{0.4}$, $GMCA_{0.45}$, and $GMCA_{0.5}$ mixes all fall below 2000 kg/m³. In contrast, $GNCA_{0.4}$, $GNCA_{0.45}$, and $GNCA_{0.5}$ fall within the range of 2300 to 2500 kg/m³. Consequently, the GMCA mixes can be categorized as lightweight concrete.

$GMCA_{0.4}$, $GMCA_{0.45}$, and $GMCA_{0.5}$ exhibit higher compressive strength compared to $GNCA_{0.4}$, $GNCA_{0.45}$, and $GNCA_{0.5}$. Specifically, the compressive strength of $GMCA_{0.4}$, $GMCA_{0.45}$, and $GMCA_{0.5}$ is 2.58%, 1.41%, and 0.82% higher than that of $GNCA_{0.4}$, $GNCA_{0.45}$, and $GNCA_{0.5}$, respectively,

at 7 days. At 28 days, the corresponding increase is 2.28%, 1.00%, and 0.67%. Moreover, the compressive strength of $GMCA_{0.4}$, $GMCA_{0.45}$, and $GMCA_{0.5}$ is 2.18%, 0.78%, and 0.48% higher than $GNCA_{0.4}$, $GNCA_{0.45}$, and $GNCA_{0.5}$, respectively, at 90 days. This observed trend can be ascribed to the voids nature of MCA, which promotes improved bonding between the mortar paste and the ITZ. This phenomenon offers a plausible explanation for the slight increase in compressive strength in GMCA than GNCA.

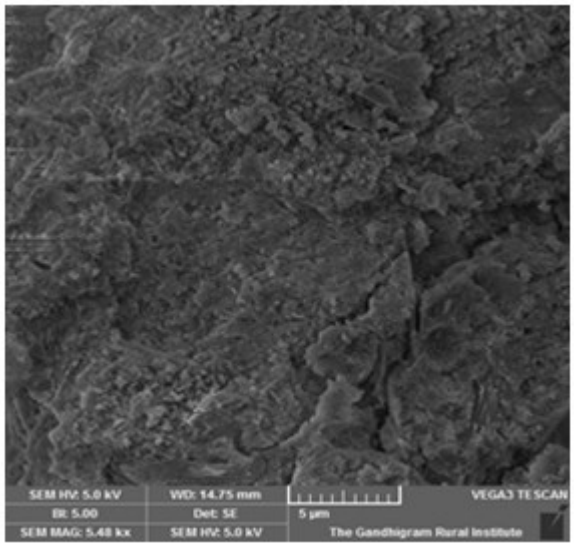

Figure 9. SEM image of $GMCA_{0.5}$ mix

The UPV for $GMCA_{0.4}$, $GMCA_{0.45}$, and $GMCA_{0.5}$ falls within the range of 4.1 to 4.3 km/s, at 7 days. By the 28th day, these values increase to a range of 4.3 to 4.5 km/s, at 90 days, the UPV for $GMCA_{0.4}$, $GMCA_{0.45}$, and $GMCA_{0.5}$ ranges from 4.4 to 4.55 km/s. According to IS 13311 (Part I): 1992, all these UPV values were classified as "Good". Notably, as the concrete ages, there was a tendency for the UPV to increase. This observation can be attributed to the reduced ITZ gap, facilitated by the angular shape of MCA and the geopolymer paste.

$GMCA_{0.4}$, $GMCA_{0.45}$, and $GMCA_{0.5}$ display RCPT values ranging from 1286 coulombs to 1371 coulombs. By the 28th day, these values range from 1201 coulombs to 1282 coulombs, at 7 days, and at 90 days, RCPT values vary from 1087 coulombs to 1140 coulombs. Importantly, all these values were categorized as "moderate" according to ASTM C 1202-17. This finding suggests that GNCA exhibits lower charge passage than GMCA. The elevation in chloride permeability can be chiefly attributed to the porous paste structure resulting from the incorporation of MCA.

$GMCA_{0.4}$, $GMCA_{0.45}$, and $GMCA_{0.5}$ demonstrate elevated sorptivity values when compared to $GNCA_{0.4}$, $GNCA_{0.45}$, and $GNCA_{0.5}$. Specifically, at 7 days, the sorptivity values for $GMCA_{0.4}$, $GMCA_{0.45}$, and $GMCA_{0.5}$ are 3.75%, 4.87%, and 5.95% higher than those of $GNCA_{0.4}$, $GNCA_{0.45}$, and $GNCA_{0.5}$, respectively. At 28 days, this difference increases to 3.00%, 4.10%, and 5.40%. Additionally, at 90 days, the sorptivity values of $GMCA_{0.4}$, $GMCA_{0.45}$, and $GMCA_{0.5}$ exceed those of $GNCA_{0.4}$, $GNCA_{0.45}$, and $GNCA_{0.5}$ by 1.75%, 3.33%, and 4.91%, respectively. The identified trend suggests that introducing MCA into geopolymer mixes results in the creation of a porous paste structure and a less favourable interfacial zone. As a consequence, this leads to increased permeability compared to NCA in geopolymer mixes.

The interaction of MCA and the geopolymer paste contributed to higher hardness values. Additionally, the GMCA mix at a L/B ratio of 0.4 achieved an improved ITZ. This improvement is further supported by the presence of a disconnected micro crack path, enhancing the concrete's capability to withstand heavier loads.

Hence, the development of lightweight geopolymer aggregates emerges as a distinctive material with versatile applications aimed at minimizing the reliance on natural aggregates. This approach not only contributes to environmental benefits by lessening the dead load of structures but also helps in lowering CO_2 emissions.

Acknowledgment

The authors wish to acknowledge Department of Civil Engineering, K.S.Rangasamy College of Technology, Namakkal, Tamil Nadu; Vivekananda College of Technology for Women, Elayampalayam, Namakkal, Tamil Nadu for the facility and support extended for the research work.

References

Albidah, A., Alghannam, M., Abbas, H., Almusallam, T. and Al-Salloum, Y. (2021). Characteristics of metakaolin-based geopolymer concrete for different mix design parameters, *Journal of Materials Research and Technology*, **10**, 84–98. https://doi.org/10.1016/j.jmrt.2020.10.027

Alqahtani, F.K., Ghataora, G., Dirar, S., Khan, M.I. and Zafar, I. (2018). Experimental study to investigate the engineering and durability performance of concrete using synthetic aggregates, *Construction and Building Materials*, **173**, 350–358. https://doi.org/10.1016/j.conbuildmat.2018.04.030

Amin, M., Tayeh, B.A., Kandil, M.A., Agwa, I.S. and Abdelmagied, M.F. (2022). Effect of rice straw ash and palm leaf ash on the properties of ultrahigh-performance concrete, *Case Studies in Construction Materials*, **17**. https://doi.org/10.1016/j.cscm.2022.e01266

Ankur, M. and Rafat, S. (2016), An overview of geopolymers derived from industrial by-product, *Construction and Building Materials*, **127**, 183–198. https://doi.org/10.1016/j.conbuildmat.2016.09.136

Baskar, P., Annadurai, S., Sekar, K. and Prabakaran, M. (2023), A review on fresh, hardened, and microstructural properties of fibre-reinforced geopolymer concrete, *Polymers*, **15** (6). 1484, https://doi.org/10.3390/polym15061484

Bekkeri, G.B., Shetty, K.K. and Nayak, G. (2023), Synthesis of artificial aggregates and their impact on performance of concrete: a review, *Journal of Material Cycles and Waste Management*, **25** (4), 1988–2011. https://doi.org/10.1007/s10163-023-01797-0

Chindaprasirt, P. (2020), Use of construction and demolition waste (CDW) for alkali-activated or geopolymer concrete, *In Advances in Construction and Demolition Waste Recycling, Elsevier*, pp. 385–403. https://doi.org/10.1016/b978-0-12-819055-5.00019-x

Chindaprasirt, P., Chareerat, T. and Sirivivatnanon, V. (2007). Workability and strength of coarse high calcium fly ash geopolymer, *Cement and Concrete Composites*, **29** (3), 224–229. https://doi.org/10.1016/j.cemconcomp.2006.11.002

Cioffi, R., Colangelo, F., Montagnaro, F. and Santoro, L. (2011), Manufacture of artificial aggregate using MSWI bottom ash,

Waste Management, **31** (2), 281–288. https://doi.org/10.1016/j.wasman.2010.09.014

Farahani, J.N., Shafigh, P., Alsubari, B., Shahnazar, S. and Mahmud, H.B. (2017), Engineering properties of lightweight aggregate concrete containing binary and ternary blended cement, *Journal of Cleaner Production*, **149**, 976–988. https://doi.org/10.1016/j.jclepro.2017.02.098

Franus, M., Barnat-Hunek, D. and Wdowin, M. (2015), Utilization of sewage sludge in the manufacture of lightweight aggregate, *Environmental Monitoring and Assessment*, **188**. https://doi.org/10.1007/s10661-015-4885-5

George, G.K. and Revathi, P. (2020), Production and utilization of artificial coarse aggregate in concrete—a review, *IOP Conference Series: Materials Science and Engineering*, **936**, 12035. https://doi.org/10.1088/1757-899X/936/1/012035

Golafshani, E., Khodadadi, N., Ngo, T., Nanni, A. and Behnood, A. (2024) Modelling the compressive strength of geopolymer recycled aggregate concrete using ensemble machine learning, *Advances in Engineering Software*, **191**, 103611. https://doi.org/10.1016/j.advengsoft.2023.103611

Gonzalez-Corrochano, B., Alonso-Azcarate, J. and Rodas, M. (2009), Production of lightweight aggregates from mining and industrial wastes, *Journal of Environmental Management*, **90** (8), 2801–2812. https://doi.org/10.1016/j.jenvman.2009.03.002

Guneyisi, E., Gesoglu, M., Ghanim, H., Ipek, S. and Taha, I. (2016). Influence of the artificial lightweight aggregate on fresh properties and compressive strength of the self-compacting mortars, *Construction and Building Materials*, **116**, 151–158. https://doi.org/10.1016/j.conbuildmat.2016.04.059

Guneyisi, E., Gesoglu, M., Pursunlu, O. and Mermerdas, K. (2013). Durability aspect of concretes composed of cold bonded and sintered fly ash lightweight aggregates, *Composites Part B: Engineering*, **53**, 258–266. https://doi.org/10.1016/j.compositesb.2013.05.036

Hajimohammadi, A., Ngo, T. and Vongsvivut, J. (2019), Interfacial chemistry of a fly ash geopolymer and aggregates, *Journal of Cleaner Production*, **231**, 980–989. https://doi.org/10.1016/j.jclepro.2019.05.232

Hao, D.L.C., Abd Razak, R., Kheimi, M., Yahya, Z., Abdullah, M.M.A.B., Burduhos Nergis, D.D., Fansuri, H., Ediati, R., Mohamed, R. and Abdullah, A. (2022), Artificial lightweight aggregates made from pozzolanic material: A review on the method, physical and mechanical properties, thermal and microstructure, *Materials*, **15** (11), 3929. https://doi.org/10.3390/ma15113929

Hardjito, D., Wallah, S.E., Sumajouw, D.M.J. and Rangan, B.V. (2004). On the development of fly ash-based geopolymer concrete, *Materials Journal*, **101**(6), 467–472. https://doi.org/10.14359/13327

Jalal, F.E., Mulk, S., Memon, S.A., Jamhiri, B. and Naseem, A. (2021). Strength, hydraulic, and microstructural characteristics of expansive soils incorporating marble dust and rice husk ash, *Advances in Civil Engineering*, 1–18. https://doi.org/10.1155/2021/8388810

Kalinowska-Wichrowska, K., Pawluczuk, E., Bołtryk, M. and Nietupski, A. (2022). Geopolymer concrete with lightweight artificial aggregates, *Materials*, **15**(9), 3012. https://doi.org/10.3390/ma15093012

Kipsanai, J.J., Wambua, P.M., Namango, S.S. and Amziane, S. (2022), A review on the incorporation of diatomaceous earth as a geopolymer-based concrete building resource, *Materials*, **15** (20), 7130. https://doi.org/10.3390/ma15207130

Kumar, P., Pankar, C., Manish, D. and Santhi, A.S. (2018), Study of mechanical and microstructural properties of geopolymer concrete with GGBS and Metakaolin, *Materials Today: Proceedings*, **5** (14), 28127–28135. https://doi.org/10.1016/j.matpr.2018.07.002

Law, D.W., Adam, A.A., Molyneaux, T.K., Patnaikuni, I. and Wardhono, A. (2015). Long term durability properties of class F fly ash geopolymer concrete, *Materials and Structures*, **48**, 721–731. https://doi.org/10.1617/s11527-014-0295-1

Lee, T.G. and Lee, J.H. (2020). Assessment of strength development at hardened stage on high-strength concrete using NDT, *Applied Sciences*, **10**, 6261. https://doi.org/10.3390/app10186261.

Lima, C., Caggiano, A., Faella, C., Martinelli, E., Pepe, M. and Realfonzo, R. (2013). Physical properties and mechanical behaviour of concrete made with recycled aggregates and fly ash, *Construction and Building Materials*, **47**, 547–559. https://doi.org/10.1016/j.conbuildmat.2013.05.015

Liu, M., Wang, C., Bai, Y. and Xu, G. (2018), Effects of sintering temperature on the characteristics of lightweight aggregate made from sewage sludge and river sediment, *Journal of Alloys and Compounds*, **748**, 522–527. https://doi.org/10.1016/j.jallcom.2018.03.211.

Liu, M.Y.J., Alengaram, U.J., Jumaat, M.Z. and Mo, K.H. (2014), Evaluation of thermal conductivity, mechanical and transport properties of lightweight aggregate foamed geopolymer concrete, *Energy and Buildings*, **72**, 238–245. https://doi.org/10.1016/j.enbuild.2013.11.047.

Lo, L.Y., Cui, H., Memon, S. and Noguchi, T. (2016), Manufacturing of sintered lightweight aggregate using high-carbon fly ash and its effect on the mechanical properties and microstructure of concrete, *Journal of Cleaner Production*, **112**, 753–762. https://doi.org/10.1016/j.jclepro.2015.08.074

Mohan, A.B. and Vasudev, R. (2018), Artificial lightweight aggregate through cold bonding pelletization of fly ash: A review, *International Research Journal of Engineering and Technology*, **5**, 778–783.

Mohmmad, S.H., Shakor, P., Muhammad, J.H., Hasan, M.F. and Karakouzian, M. (2023), Sustainable alternatives to cement: synthesizing metakaolin-based geopolymer concrete using nano-silica, *Construction Materials*, **3** (3), 276–286. https://doi.org/10.1016/j.conmat.2023.06.004

Nadesan, M.S. and Dinakar, P. (2018), Influence of type of binder on high-performance sintered fly ash lightweight aggregate concrete, *Construction and Building Materials*, **176**, 665–675. https://doi.org/10.1016/j.conbuildmat.2018.01.158

Okoye, F.N., Prakash, S. and Singh, N.B. (2017), Durability of fly ash-based geopolymer concrete in the presence of silica fume, *Journal of Cleaner Production*, **149**, 1062–1067. https://doi.org/10.1016/j.jclepro.2017.02.174

Ollivier, J.P., Maso, J.C. and Bourdette, B. (1995). Interfacial transition zone in concrete, *Advanced Cement-Based Materials*, **2** (1), 30–38. https://doi.org/10.1016/1065-7355(95)00016-3

Ouda, A.S. and Gharieb, M. (2020), Development of the properties of brick geopolymer pastes using concrete waste incorporating dolomite aggregate, *Journal of Building Engineering,* **27**. https://doi.org/10.1016/j.jobe.2019.100919

Pawluczuk, E., Kalinowska-Wichrowska, K., Jimenez, J.R., Fernández-Rodríguez, J.M. and Suescum-Morales, D. (2021). Geopolymer concrete with treated recycled aggregates: Macro

and microstructural behavior, *Journal of Building Engineering*, **44**, 103317. https://doi.org/10.1016/j.jobe.2021.103317.

Peng, Z., Shi, C., Shi, Z., Lu, B., Wan, S., Zhang, Z., Chang, J. and Zhang, T. (2020). Alkali-aggregate reaction in recycled aggregate concrete, *Journal of Cleaner Production*, **255**, 120238. https://doi.org/10.1016/j.jclepro.2020.120238

Pham, T.M., Lim, Y.Y., Pradhan, S.S. and Kumar, J. (2021). Performance of rice husk ash-based sustainable geopolymer concrete with ultra-fine slag and corn cob ash, *Construction and Building Materials*, **279**, 122526. https://doi.org/10.1016/j.conbuildmat.2021.122526.

Prasad, B.V.V., Paul Daniel, A. and Yadav, S.K. (2022), Strength and microstructure behaviour of high calcium fly ash based sustainable geopolymer concrete, *Journal of Engineering, Design and Technology*, **20** (2), 436–454. https://doi.org/10.1108/JEDT-12-2021-0363

Priyanka, M., Karthikeyan, M. and Sri Rama Chand, M. (2020). Development of mix proportions of geopolymer lightweight aggregate concrete with LECA, *Materials Today: Proceedings*, **27**, 958–962. https://doi.org/10.1016/j.matpr.2020.04.213

Qian, L.-P., Huang, B.-T., Xu, L.-Y. and Dai, J.-G. (2023). Concrete made with high-strength artificial geopolymer aggregates: Mechanical properties and failure mechanisms, *Construction and Building Materials*, **367**, 130318. https://doi.org/10.1016/j.conbuildmat.2023.130318

Ralli, Z.G. and Pantazopoulou, S.J. (2021), State of the art on geopolymer concrete, *International Journal of Structural Integrity*, **12** (4), 511–533. https://doi.org/10.1108/IJSI-03-2021-0017

Ren, X. and Zhang, L. (2018), Experimental study of interfacial transition zones between geopolymer binder and recycled aggregate, *Construction and Building Materials*, **167**, 749–756. https://doi.org/10.1016/j.conbuildmat.2018.02.111

Sagar, B. and Sivakumar, M.V.N. (2021), Use of alccofine-1203 in concrete: review on mechanical and durability properties, *International Journal of Sustainable Engineering*, **14**(6), 2060–2073. https://doi.org/10.1080/19397038.2021.1938708

Shi, C., Qu, B. and Provis, J.L. (2019), Recent progress in low-carbon binders, *Cement and Concrete Research*, **122**, 227–250. https://doi.org/10.1016/j.cemconres.2019.05.009

Shi, X.S., Collins, F.G., Zhao, X.L. and Wang, Q.Y. (2012), Mechanical properties and microstructure analysis of fly ash geopolymeric recycled concrete, *Journal of Hazardous Materials*, 20–29. https://doi.org/10.1016/j.jhazmat.2012.07.070

Tajra, F., Elrahman, M.A., Chung, S.-Y. and Stephan, D. (2018), Performance assessment of core-shell structured lightweight aggregate produced by cold bonding pelletization process, *Construction and Building Materials*, **179**, 220–231. https://doi.org/10.1016/j.conbuildmat.2018.05.269

Thokchom, S., Ghosh, P. and Ghosh, S. (2009), Effect of water absorption, porosity and sorptivity on durability of geopolymer mortars, *ARPN Journal of Engineering and Applied Sciences*, **4** (7), 28–32.

Un, C.H., Sanjayan, J.G., San Nicolas, R. and Van Deventer, J.S.J. (2015). Predictions of long-term deflection of geopolymer concrete beams, *Construction and Building Materials*, 94, 10–19. https://doi.org/10.1016/j.conbuildmat.2015.06.064

Vargas, P., Restrepo-Baena, O. and Tobón, J.I. (2017). Microstructural analysis of interfacial transition zone (ITZ) and its impact on the compressive strength of lightweight concretes, *Construction and Building Materials*, **137**, 381–389. https://doi.org/10.1016/j.conbuildmat.2017.01.129

Verma, M., Dev, N., Rahman, I., Nigam, M., Ahmed, M. and Mallick, J. (2022). Geopolymer concrete: a material for sustainable development in Indian construction industries, *Crystals*, **12**(4), 514. https://doi.org/10.3390/cryst12040514

Wang, B., Yan, L., Fu, Q. and Kasal, B. (2021), A comprehensive review on recycled aggregate and recycled aggregate concrete, *Resources, Conservation and Recycling*, **171**, 105565. https://doi.org/10.1016/j.resconrec.2021.105565

Wang, D., Cui, C., Chen, X.-F., Zhang, S. and Ma, H. (2020), Characteristics of autoclaved lightweight aggregates with quartz tailings and its effect on the mechanical properties of concrete, *Construction and Building Materials*, **262**, 120110. https://doi.org/10.1016/j.conbuildmat.2020.120110

Xie, J., Wang, J., Rao, R., Wang, C. and Fang, C. (2019), Effects of combined usage of GGBS and fly ash on workability and mechanical properties of alkali activated geopolymer concrete with recycled aggregate, *Composites Part B: Engineering*, **164**, 179–190. https://doi.org/10.1016/j.compositesb.2018.11.067

Xu, L.-Y., Qian, L.-P., Huang, B.-T. and Dai, J.-G. (2021), Development of artificial one-part geopolymer lightweight aggregates by crushing technique, *Journal of Cleaner Production*, **315**, 128200. https://doi.org/10.1016/j.jclepro.2021.128200

Yuvaraj, K., and Ramesh, S. (2022), Performance study on strength , morphological , and durability characteristics of coal pond ash concrete, *International Journal of Coal Preparation and Utilization*, 1–15. https://doi.org/10.1080/19392699.2022.2101457

Zhang, Y. and Aslani, F. (2021), Compressive strength prediction models of lightweight aggregate concretes using ultrasonic pulse velocity, *Journal of Construction and Building Materials*, **292**, 123419. https://doi.org/10.1016/j.conbuildmat.2021.123419

Zheng, Y., Zhang, Y. and Zhang, P. (2021), Methods for improving the durability of recycled aggregate concrete: A review, *Journal of Materials Research and Technology*, 15, 6367–6386. https://doi.org/10.1016/j.jmrt.2021.03.016

Zhuang, X.Y., Chen, L., Komarneni, S., Zhou, C.H., Tong, D.S., Yang, H.M., Yu, W.H. and Wang, H. (2016), Fly ash-based geopolymer: Clean production, properties and applications, *Journal of Cleaner Production*, **125**, 253–267. https://doi.org/10.1016/j.jclepro.2016.03.019

Zong, L., Fei, Z. and Zhang, S. (2014), Permeability of recycled aggregate concrete containing fly ash and clay brick waste, *Journal of Cleaner Production*, **70**, 175–182. https://doi.org/10.1016/j.jclepro.2014.01.019